Organic Carbon Isotope Stratigraphy of the Karoo Supergroup

17

Maarten J. de Wit

Abstract

Carbon isotopes are being used increasingly for high resolution chemostratigraphy. $\delta^{13}C$ variations provide relative temperature scales that can be complemented with litho- and bio-stratigraphy to reconstruct local ecosystem and global climate shifts. We present the first Karoo terrestrial organic carbon isotope curve, calibrated against U/Pb zircon dates from interbedded ash-fall tuffs, which can be used for correlation between separate terrestrial Gondwana basins and with marine sequences elsewhere. We identify a number of distinct shifts in the carbon isotope stratigraphy of the Karoo and explore these to discuss punctuated and gradational changes linked to local paleoenvironments and global climates, from polar to desert conditions, over a span of about 200 million years that includes two major extinction events.

Keywords

Terrestrial chemical stratigraphy • Carbon isotopes • Climate • Ecosystem fluctuations

17.1 Introduction

Terrestrial sequences are difficult to correlate with their marine counterparts (Ager 1973). Traditional stratigraphic tools based on palaeontology from these different paleo-ecosystems need independent data to verify stratigraphic equivalence, and common calibrated standards are scarce. Chrono-stratigraphy using radiometric age dating often depends on the presence in both environments of contemporaneous volcanic material with igneous minerals that can be dated with confidence, but volcanic events are rarely frequent or regional enough to provide detailed resolution. Magneto-stratigraphy can best resolve some of these issues, but primary paleo-magnetic signatures may be re-magnetised during diagenesis, basin fluid-flow and low-grade metamorphism, particularly in Paleozoic sequences (McCabe and Elmore 1989; Smith 1999). Such secondary effects have, for example, reset the magnetic fingerprints of large sections of the Karoo Basin sediments (Bachtadse et al. 1987; Opdyke et al. 2001; Ward et al. 2005).

More recently, chemical stratigraphy has been explored as a tool for geological correlations, particularly using strontium, carbon and oxygen isotopes (e.g., Veizer et al. 1999; Grossman 1994). In the case of strontium isotopes, however, marine and terrestrial sequences are buffered through their very different oceanic and terrestrial fluid-rock reservoirs, respectively, and are therefore not useful as stratigraphic tools to correlate between marine and terrestrial environments. On the other hand, light stable isotopes of carbon and oxygen isotopes acquire equilibrium between hydrosphere reservoirs and the atmosphere within a relative short space of time (e.g., Ruddiman 2000). For all practical stratigraphy purposes, isotopic ratios of carbon and oxygen in marine and terrestrial environments change in tandem and are recorded, by proxy, in their respective biomass. Variations in isotope ratios of carbon in organic matter and

With contributions from AEON research associates James Alexander, John Decker, Joy Ghosh, Nicolas Rakotosolofo, and Stephanie de Villiers.

M.J. de Wit (✉)
AEON, Africa Earth Observatory Network, Nelson Mandela Metropolitan University, Port Elizabeth, South Africa
e-mail: maarten.dewit@nmmu.ac.za

B. Linol and M.J. de Wit (eds.), *Origin and Evolution of the Cape Mountains and Karoo Basin*,
Regional Geology Reviews, DOI 10.1007/978-3-319-40859-0_17

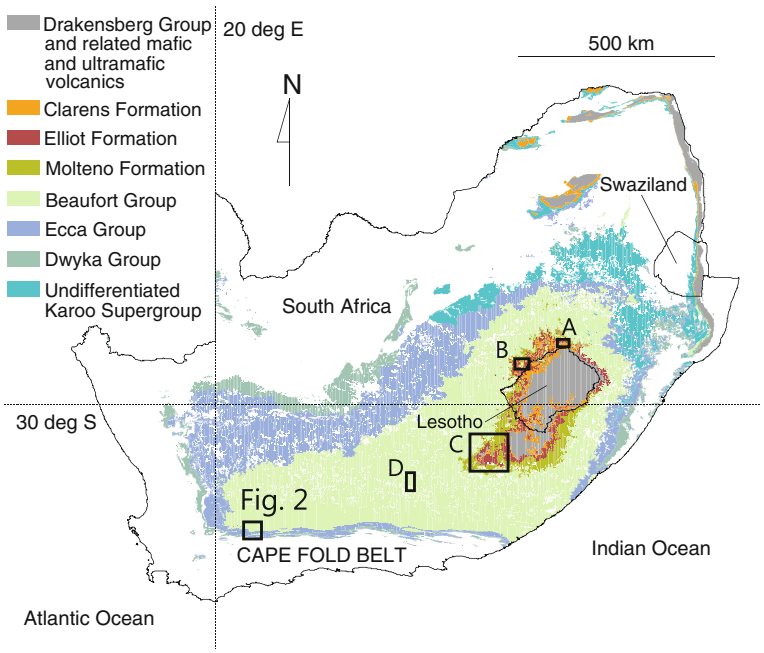

Fig. 17.1 Simplified geology of the Karoo Basin (outcrop map) with sampled locations *(squares)*. A = Emeus, near Golden Gate; B = Bramleyshoek; C = Region of Molteno fossil sites sampled from the Anderson Collection (see text); D = P-T boundary along the Lootberg Pass. Details of Waaipoort-Dwyka-lower Beaufort sections near Laingsburg are shown in Fig. 17.2

carbonates can potentially therefore provide reliable signatures for stratigraphic correlations between terrestrial and marine sequences. This has been used successfully, for example, to correlate repeated marine incursions in Jurassic terrestrial sediments (Jenkyns et al. 2002) and to track the history of Cenozoic glaciations on a global scale using marine sediments and terrestrial ice cores (e.g., Raymo 1994), respectively.

Plants in different terrestrial environments use the same atmospheric chemistry to photosynthesise, and isotopic fractionation of carbon isotopes during photosynthesis is well understood. Therefore, variations in the ratio of organic carbon isotopes of fossil organic remains (or penecontemporaneous carbonates) in sediments (e.g., $^{12}C/^{13}C$, expressed as $\delta^{13}C_{org}$) are useful proxy for changes in coupled atmospheric/oceanic/biosphere conditions related, for example, to global climate change (e.g., Berner 1990; Faure et al. 1995; de Wit et al. 2002). Although fractionation differs between plants that use different photosynthetic pathways, it is generally agreed that before 200 Ma only one type of photosynthetic pathway (C3) had evolved. The organic carbon isotope signatures of Karoo fossil plant materials are therefore usually relatively simple to interpret (Ghosh 1999; de Wit et al. 2002; Decker 2004; Decker and de Wit 2005), and can thus provide a powerful tool to facilitate regional correlation of terrestrial sequences, and to track details of climate changes during evolution of this Gondwana continental interior that was first covered by Antarctic-like ice caps in the Carboniferous and then by Sahara-like dune fields in the Jurassic-Cretaceous, a period of more than 200 million years (see Preface of this book).

This chapter summarises the organic carbon isotope stratigraphy of the Karoo Supergroup across three sequences across the Karoo Basin (Fig. 17.1). The first comprises the Lower Karoo (Carboniferous-Permian) around Laingsburg in the southwest Karoo Basin; the second covers the Upper Karoo (Triassic-Jurassic) from a number of localities in the central sector of the Karoo Basin. These two sequences are linked through a short third sequence across the Permian-Triassic (P-T) boundary (presently dated at 252.17 ± 0.06 Ma; Burgess et al. 2014) in the south-central Karoo exposed around Graaff-Reinet (along the Lootsberg Pass), and which has been sampled also for Carbon isotopes by several other research groups (see for example Chap. 15 of this book).

17.2 Selected Sequences

The first sequence is well-exposed between the contacts of the Lower Paleozoic Cape Supergroup and the overlying Upper Paleozoic part of the Beaufort Group (Fig. 17.2). It represents a near complete sequence from the Upper Carboniferous Waaipoort Formation (upper most Witteberg Group of the Cape Supergroup) to the Middle Permian Waterford-Beaufort boundary of the Karoo Supergroup, and includes the classic Permo-Carboniferous glacial deposits of the Dwyka Group (du Toit 1926; Visser 1987). Of particular interest is to test for climate variation during the time of deposition of the Dwyka Group.

The second sequence traces the organic isotope stratigraphy of the Mesozoic upper Karoo Supergroup. This

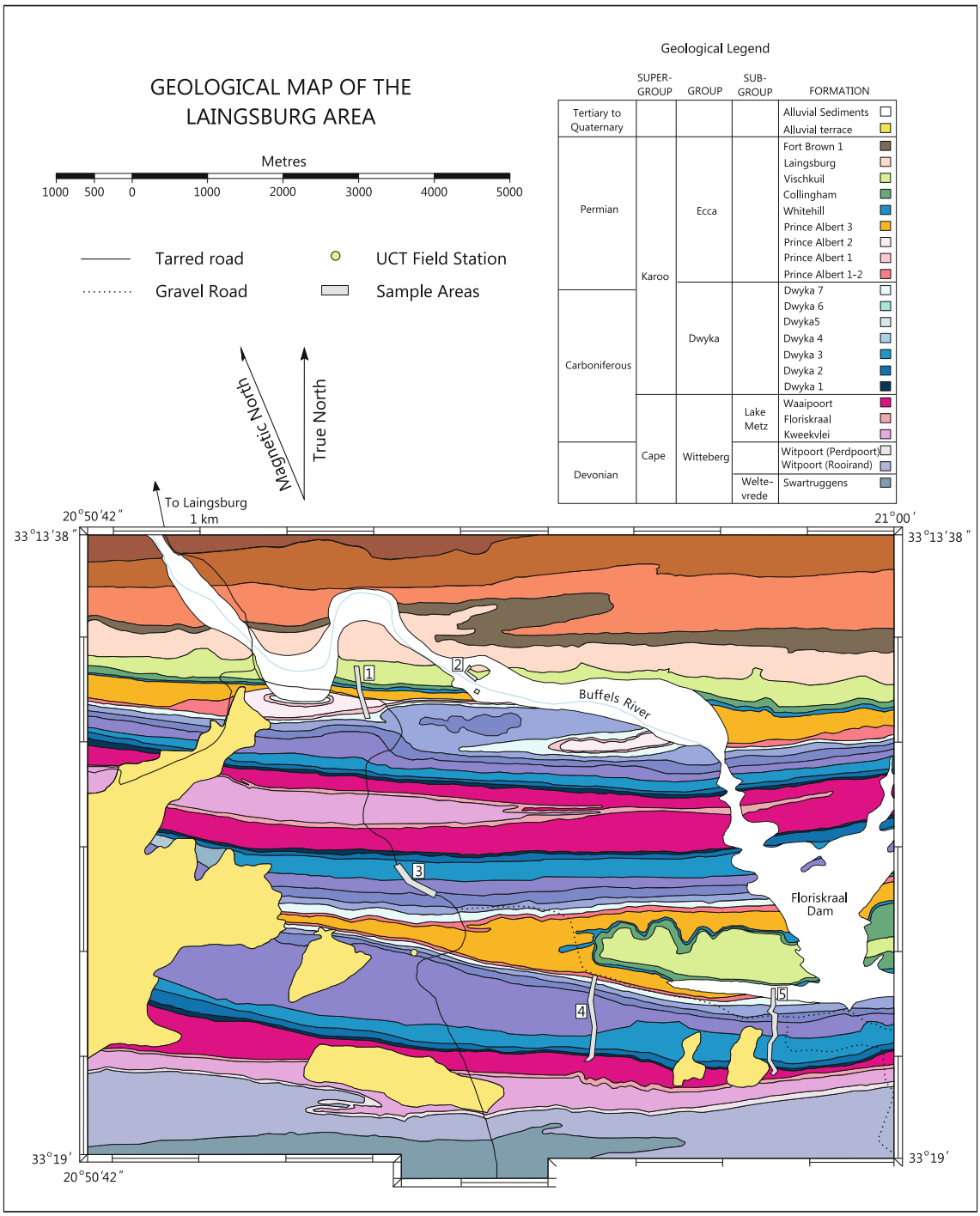

Fig. 17.2 Geological map of the field area south of Laingsburg (modified from Knütter et al. 1995 and Alexander 1999)

sequence is directly overlain by the continental flood basalts of the Jurassic Drakensberg lavas that have been dated at 182–183 Ma (Duncan et al. 1997), and thus limits the upper-bound of our terrestrial organic carbon isotope history to the Lower Jurassic. This carbon isotope curve is derived from plant and insect fossils from the Molteno, Elliot and Clarens Formations, deposited under conditions of increasing aridity from the Late Triassic into the Early Jurassic (Anderson et al. 1999).

Our third $\delta^{13}C_{org}$ section links the lower and upper Karoo sections through the P-T transition in the Beaufort Group, which is based predominantly on vertebrates (Day et al. 2015). Attempts to record the $\delta^{13}C_{org}$ across the P-T boundary of the Karoo Basin have yielded contrasting

results. A gradual negative trend over nearly 20 myrs leading up to the P-T boundary was first identified from different parts of basin using apatite from tusks of the mammal-like reptile *Dicynodon* (as a proxy for the contemporaneous vegetation of these herbivores) and from boreholes through coal-bearing sequences (Thackeray et al. 1990; Faure et al. 1995). Both these studies conclude that the start of a gradual decline in $\delta^{13}C_{org}$ was well on the way before the P-T boundary. A subsequent study of $\delta^{13}C_{carb}$ from carbonate nodules conducted at three nearby sites (Doornplaats, Lootsberg and Bethulie) gave conflicting results (MacLeod et al. 2000), some attributed to secondary alterations (de Wit et al. 2002). We re-examined the Lootsberg section for organic materials preserved in the carbonate nodules. More recent work along detailed lithologic and palaeontological sections (e.g., Gastaldo et al. 2015) is reported in Chap. 15, and is not described further here.

17.3 Geological Background

17.3.1 The Lower Karoo Supergroup: Dwyka to Beaufort Groups

Lithostratigraphic and palynology evidence suggest that the onset of glaciation was in progress during deposition of the uppermost Witteberg Group (the Tournasian Waaipoort Formation; see also Chap. 13 in this book) and that there is minimal hiatus before glaciers advanced across a Witteberg glaciogene surface (Streel and Theron 1999). Thereafter glaciogenic sedimentation and erosion dominated until well into the Early Permian (~288 Ma; Artinskian) accumulating up to 800 m of Dwyka Group diamictites and rhythmites in the southern part of the Karoo Basin, and classical striated pavements along the northern fringes of the basin, respectively (Du Toit 1926; Visser 1987). Local ice-flow directions indicate provenances to the north (Chap. 9 in this book). Between the Early to Late Carboniferous, the South Pole moved from southern Africa to Antarctica; and the northern margins of the ice sheets reached as far as Tanzania, Madagascar, the Central African Republic and Angola (Linol et al. 2016; see Preface of this book). Visser (1987) estimated an ice sheet cover of more than 4 km above the basin floor, similar to that of large parts of present-day East Antarctica.

Whereas many investigators infer a marine setting for the deposition of these diamictites and related varves (e.g., McLachland and Anderson 1973; Johnson et al. 1997 and references therein), there is no unequivocal evidence for this. Marine fossils occur only at the top of the Dwyka along the western margins of the basin, particularly in southern Namibia (Warmbath Basin) and along the deep glacial valley through the Vryburg-Prieska region along the northern extents of the Karoo Basin. These are witness of a short marine transgression at the end of the glaciation (Visser 1987). By contrast, terrestrial plant fragments are common throughout the Karoo Basin, albeit rare in the Dwyka (Plumstead 1964; see also Chap. 16 in this book). It is therefore possible that the entire Dwyka sequence of the Karoo Basin was deposited in a terrestrial setting (du Toit 1926), including those of the overlying organic-rich mudstones of the Prince Albert, Whitehill and Collingham Formations (see Higgs 2010 and references therein; also Chaps. 10 and 11 this book), during which the Karoo Basin may have become a gigantic inland lake up to three times the size of the present Black Sea (e.g., Faure and Cole 1999). These observations imply that during early Dwyka times, the water-lain diamictites may represent glaciogenic lake-sediments deposited peripheral and beneath the major continental ice cap of Gondwana (de Wit et al. in prep).

Two occurrences of rhyolitic-andesitic volcanic tuff are present in the Dwyka Group of southern Africa (Bangert et al. 1999). These were most likely derived from a magmatic arc to the south (Bangert et al. 1999; Linol et al. 2016). U/Pb dating on zircons from tuffs near Laingsburg about 400 m above the base of the Dwyka has yielded a date of 297 ± 1.8 Ma (Bangert et al. 1999). The age of the top of the Dwyka has been similarly derived using zircons dates from tuffs in the lowermost beds of the overlying Prince Albert Formation (288 ± 3 and 289 ± 3.8 Ma). Thus, the Dwyka Group in the southern Karoo Basin spans about 50 million years, with the upper 200 m representing less than 10 million years, or at most 20 ‰ of the glacial period.

Following rapid disintegration of the ice cap at about 290 Ma (Asselian-Sakmarian), glaciogenic sedimentation gave way to slow deposition of black suspended muds of the Prince Albert and Whitehill Formations (for further details see Chaps. 10 and 11 in this book). Geochemistry (Zawada 1988; Faure and Cole 1999) suggests that most of these deposits are fresh to brackish water lake deposits, and a 'Baltic Sea' model has recently been suggested to account for this (see Chap. 10 in this book), and which by then extended across into the Paraná Basin of South America as a gigantic lacustrine basin (Chap. 18 in this book).

The Whitehill Formation, with its characteristic fauna of the fresh water *Mesausaurus* and dragonflies (du Toit 1926; see also Chap. 10 this book) is abruptly overlain by the upward coarsening sequence of turbidites of the Collingham to Laingsburg Formation and the more deltaic sequences of the Ford Brown Formation. These deposits are in turn succeeded by a succession of shore-line and in turn braided-river deposits of the Beaufort Group (see Chap. 14 in this book) that contain the terrestrial mammal-like reptiles, and the Permo-Triassic boundary (e.g., MacLeod et al. 2000; Day et al. 2015; Gastaldo et al. 2015; Chap. 15 in this book).

We use selected U/Pb zircons from tuffs at various locations across the southern Karoo (e.g., Bangert et al. 1999; Fildani et al. 2007; Rubidge et al. 2013; McKay et al. 2015; Day et al. 2015; Gastaldo et al. 2015) to further "calibrate" our $\delta^{13}C_{org}$ stratigraphy sections.

17.3.2 The Upper Karoo Supergroup: Molteno, Elliot and Clarens Formations

Karoo terrestrial sedimentary sequences terminate at the boundary with the overlying Drakensberg flood basalts, dated at 182 ± 1 Ma (Duncan et al. 1997). Formerly known as the Stormberg Group (Bordy et al. 2004), these siliciclastic formations have been interpreted to represent contemporaneous environments in a systems tract shifting towards a southerly source (Turner 1983, 1999; Smith et al. 1993; Bordy et al. 2004). No geochronological data exists for this section of the Upper Karoo Supergroup (but see Chap. 12 in this book for a date to be published soon from a tuff in the upper Elliot Formation).

The lower Molteno Formation is dominated by coarse sandstones, interbedded with grey shales and occasional seams of coal (du Toit 1926, 1954), and is thought to have been deposited by perennial, high energy, low-sinuosity braided streams (Turner 1983). It is the most productive macroflora-bearing formation in terms of both diversity and localities, offering the clearest available window globally onto the floral and insect diversity during the Late Triassic (Anderson and Anderson 2003; Anderson et al. 1999; Scott et al. 2004; see the Preface and Chap. 16 in this book). Thus, the Molteno plant and insect fossils provide the most robust $\delta^{13}C_{org}$ proxy for Late Triassic (Carnian) terrestrial environments in southern Gondwana and global atmosphere conditions.

The overlying Elliot Formation is characterised by purple and red mudstones and shales with calcareous nodules, red sandstones and thickly bedded yellow and white feldspathic sandstones (Decker 2004; Bordy et al. 2004; Chap. 12 this book). The Elliot has been interpreted as alluvial floodplain deposits with interacting fluvial and aeolian processes during increasingly arid conditions (see Bordy et al. 2004 and Decker and de Wit 2005 for references). Overlying the Elliot Formation is the Clarens Formation, dominated by massive aeolian sandstones (du Toit 1926), in addition to facies representing distal alluvial fan and playa lake environments (Smith et al. 1993; Bordy et al. 2004). The lowermost flows of the overlying Drakensberg basalts often fill the morphology of the dune fields of the Clarens Formation, and intercalation of fossiliferous Clarens strata with the overlying lavas and volcanic ashes indicates contemporaneous deposition at circa 183 Ma.

17.4 Sampling

Our samples include organic materials and host rocks cleaned of carbonates. All sampling methods, locations and data, including details of the instrumentation and analytical work, with standards and reproducibility, are described in detail elsewhere (Ghosh 1999; Alexander 1999; de Wit et al. 2002; Decker 2004; Decker and de Wit 2005).

17.5 The Lower Karoo, Laingsburg

150 samples were collected along five transects in the Laingsburg area (Dwyka and Ecca Groups; Figs. 17.1 and 17.2). Sampling was conducted at intervals of between 50 cm to 50 m depending on the litho-stratigraphy and heterogeneity of the sections. Sampling was carried out using a modified lithological map compiled by Knütter et al. (1995; Fig. 17.2). The $\delta^{13}C_{org}$ section in our study area (Fig. 17.2) is represented by about 800 m of lodgement, rain-out and subaqueous and subglacial meltwater sands, suspended mud, and turbidity current sands and silts, deposited in at least seven upward fining cycles (Units 1–7), each starting with thick coarse tillites/diamictites and terminating in thin shale horizons and rhythmites/varves.

17.6 The Permian-Triassic Transition at Lootsberg Pass

For our second section, we separated organic matter preserved in 30 soil carbonate nodules collected along the Lootsberg Pass across the P-T boundary (Fig. 17.1). Details of our sample locations and data are given in Ghosh (1999) and de Wit et al. (2002). This section, as well as other nearby sections, has been studied by numerous people, and Chap. 15 of this book provides a significant summary of the present status.

17.7 The Molteno, Elliot and Clarens Formations

For our third section, 41 Molteno Formation samples for carbon isotope analysis were obtained from the Anderson collections (Anderson and Anderson 2003), housed in National Botanical Institute (NBI), Pretoria (now relocated to the Centre for Paleosciences at University of the Witwatersrand, Johannesburg). Plant, wood, insect fossils and rock samples were obtained from eight different sites (Fig. 17.1), the detailed locations of which are shown in Decker (2004) and Decker and de Wit (2005). 15 rock samples were

collected at a short section (~17 m) across the Molteno/Elliot Formation contact near Bramleyshoek (Fig. 17.1). Outcrop is poor and the contact not well defined (see also Chap. 12 in this book). 44 samples of the Lower and Upper Elliot Formation, basal and lowermost Clarens Formation were collected near Golden Gate (Fig. 17.1).

17.8 A Preliminary Composite Chemo-Stratigraphic Profile for the Karoo Basin

Figure 17.3 is a composite plot showing the measured $\delta^{13}C_{org}$ against time-stratigraphy for the entire Karoo Basin constructed using the above-mentioned data. Selected stratigraphic heights above the lowest sample site are indicated, and from which approximate maximum sedimentation rates can be estimated (Fig. 17.4). $\delta^{13}C_{org}$ has a varied range of values, from −11 to −32 ‰, with majority of samples falling between −21 and −28 ‰. At a broad scale, the variations in $\delta^{13}C$ can be divided into at least eight regimes (I–VIII, Fig. 17.3).

Regime I covers most of the glacial deposits from upper Tournasian (~346 Ma) up until Unit 5 of the Dwyka Group (~297 Ma, lower Asselian). During this ca. 50 myrs time-interval, $\delta^{13}C$ ranges between −22 to −28 ‰ (~25 ± 3 ‰), whilst sedimentation accumulation rates were very low (Fig. 17.4). From there upward, there is a steady increase in $\delta^{13}C$ between −26 and −20 ‰ during the deglaciation period, with a simultaneous increase to higher sediment accumulation rates. The transition to Regime III starts during the last glacial deposits (Regime II), consistent with faster accumulation rates associated with extensive melting and retreat of the ice cover. These conditions terminate abruptly when sediment accumulation rate of fine detritus under anoxic conditions suddenly decreases during the Prince Albert and Whitehill times (~290–276 Ma; Regimes III and IV).

Thereafter there is a steady decrease of $\delta^{13}C$ from −21 to −23 ‰ (Regime V) during a period of high sedimentation rates following the onset of turbidite deposition of the Collingham Formation and which continues up until early Beaufort Group times, after which subaerial sedimentation establishes itself permanently for the rest of the Permian (see Preface and Chap. 14 in this book). An early phase of uplift of the proto-Cape Mountains may have occurred just after the Dwyka Group was deposited, to coincide with the regional (global) increase in burial of carbon, mostly in the form of the extensive Karoo coal deposits at shallow depths throughout Gondwana (Veevers et al. 1994; Ghosh 1999; Faure et al. 1995; de Wit et al. 2002). The $\delta^{13}C_{org}$ of Permian (lower Ecca) coal ranges between −24 and −22 ‰ (Faure et al. 1995); the average $\delta^{13}C_{org}$ in the lower Ecca gas shales of the deeper water deposits range between −24 to −18 ‰ (Fig. 17.5), within the range of −25 to −19 ‰ determined by Geel et al. (2015; see also Chap. 11 in this book).

There is a distinct negative $\delta^{13}C$ shift of about 10 ‰, at first relatively gently, increasing from about −21 to −23 ‰ during deposition of the Karoo turbidites, and thereafter more sharply (following the transition to terrestrial environments) towards the P-T boundary, just below and across which there are rapid fluctuations between −27 and −32 ‰ (Regimes V and VI; see also Thackeray et al. 1990; Faure et al. 1995, MacLeod et al. 2000; de Wit et al. 2002). Soon after the P-T boundary, $\delta^{13}C$ returns to values of around −25 to −21 ‰ by Molteno times in the Triassic (Regime VII), after which arid conditions become established (Regime VIII). Because of a significant hiatus (Regime VII), the rate of increase in $\delta^{13}C$ during the Early Triassic is not known.

17.8.1 Significant Shifts in the Lower Karoo

$\delta^{13}C_{org}$ from the Waaipoort and most of the Dwyka (Regime I) is characterised by small, distinct fluctuations, but one most striking feature of our results is the similar stratigraphic positions and extremely high $\delta^{13}C$ values of two positive spikes in Unit 2 of the Dwyka Group of about –5 and –11 ‰, respectively (Alexander 1999). Because these peaks were detected in two separate transects they likely represent genuine dramatic excursions to extreme cold conditions over a very short stratigraphic section (~25 m), followed by a dramatic return to relative cool temperatures. The actual $\delta^{13}C_{org}$ values reached, −12 to −13 ‰, are similar to that reported for organic material deposited in modern subglacial Antarctic lakes (Bell and Karl 1999; Siegert et al. 2001). It is therefore tempting to contribute this to organic material of similar nature. However, similar large single positive spikes recorded at approximately similar biostratigraphic levels of the Carboniferous sequences of the USA, Europe and Russia could also imply a global atmospheric link related to sudden burial of extensive plant materials (Saltzman et al. 2000; Mii et al. 2001). The ultimate cause of this large event will require more detailed work across the Dwyka and its Gondwana equivalents in central Africa, Madagascar, South America, India, Antarctica.

The shifts in $\delta^{13}C_{org}$ of ~4–6 ‰ over a very short stratigraphic section across the boundaries between Dwyka Units 5–7 (Regime II) could be interpreted as a possible climatic shifts from interglacial to glacial (e.g., Visser 1987). The data in regime II is not of a high enough resolution to resolve this at present. However, the rapid decrease in the $\delta^{13}C_{org}$ at the end of Unit 7 supports an interpretation of rapid climatic warming from the Dwyka to the Prince Albert Formation (see also Chap. 10 in this book). This is consistent

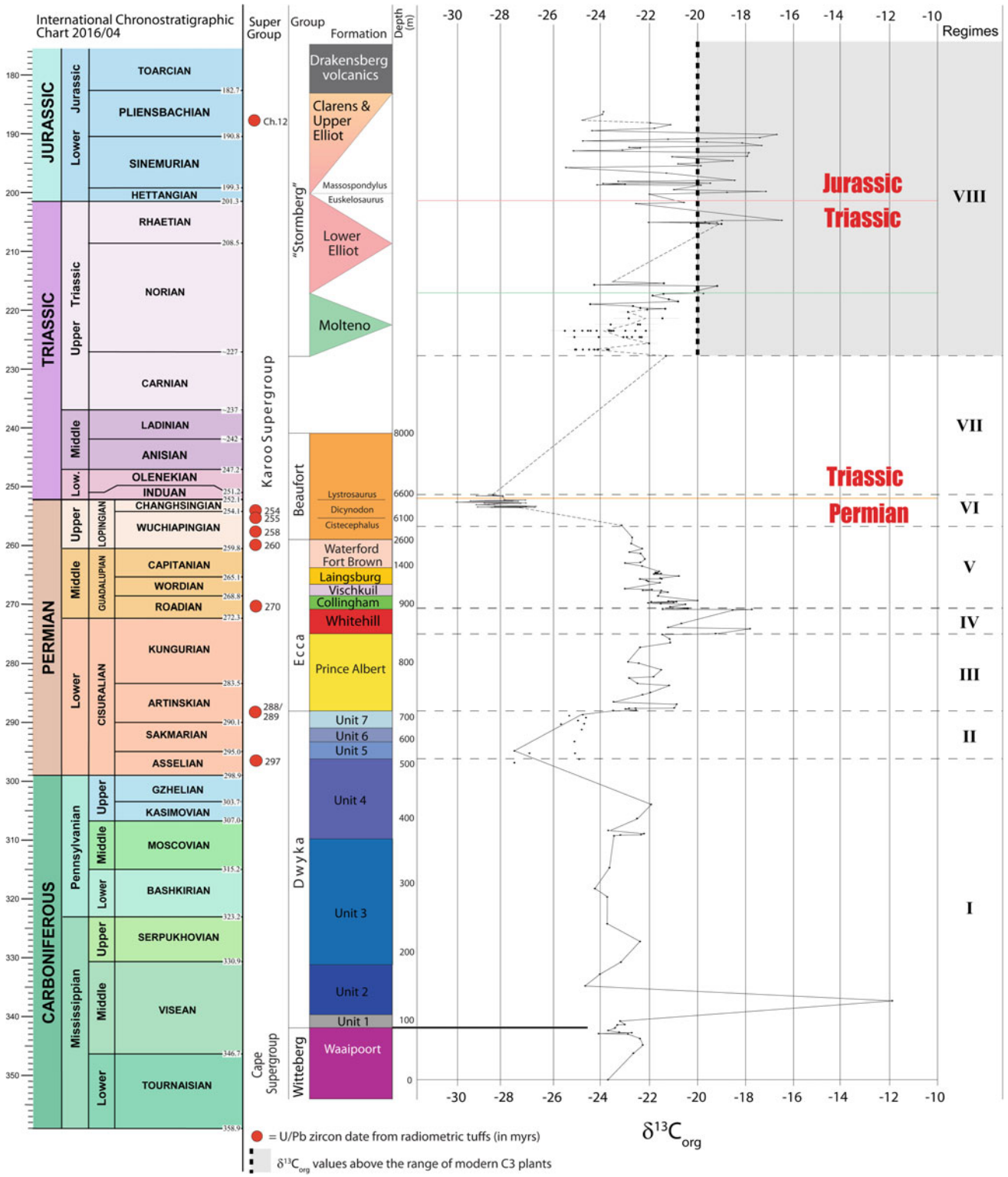

Fig. 17.3 Composite $\delta^{13}C_{org}$ stratigraphy across the south-central Karoo Basin. $\delta^{13}C_{org}$ data across the Dwyka and Ecca Groups (Regimes I–V) are from Alexander (1999) and Ghosh (1999). Data across the Permian-Triassic boundary (Regime VI) are combined from Thackeray et al. (1990); Faure et al. (1995); Gosh (1999), de Wit et al. (2002), and Ward et al. (2005), and are similar to those reported in MacLeod et al. (2000). $\delta^{13}C_{org}$ data from the Triassic sections (Regime VIII) are from Decker (2004) and Decker and de Wit (2004). See text for detailed analyses of the $\delta^{13}C_{org}$ fluctuations

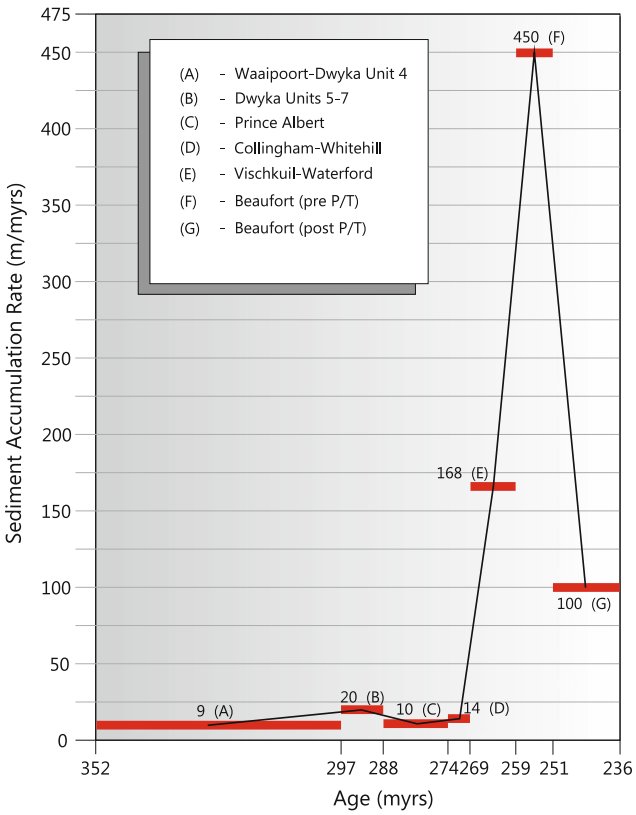

Fig. 17.4 Approximated maximum sediment accumulation rates for the Karoo Basin based on sediment thicknesses of sampled sections and U/Pb zircon dates (de Wit et al. in prep). P/T = Permian-Triassic Boundary

with the Chemical Index of Alteration (CIA) of the Karoo rocks. Dwyka diamictites have a low range of CIA values, consistent with mechanical weathering and cold conditions. By contrast, CIA values for mudrocks in the Dwyka units show wide fluctuating ranges that are interpreted to represent deposition during interglacial episodes, and shales from the overlying Prince Albert Formation have high CIA values suggesting a rapid transition to a much more intensive weathering regime and warmer climatic conditions (Visser and Young 1990).

Of significant interest, is the positive shift of 9 ‰, from −27 to −18 ‰, commencing in Dwyka Unit 5 and terminating at the end of the Whitehill Formation (Regime III/IV). This trend is consistent with increased burial of plant material and the formation/preservation of peat, coal and oil causing a shift to more positive $\delta^{13}C$ values. This period coincides with the formation of the major known coal deposits within the Karoo and other terrestrial Gondwana basins (Veevers et al. 1994; Faure et al. 1995; Ghosh 1999; de Wit et al. 2002), as well as the high TOC of the deep water black shales such as the Whitehill Formation (4.5 weight percent; Geel et al. 2015).

Although $\delta^{13}C_{org}$ variability within the Whitehill Formation (Regime IV) are clearly complex, with large (>3 ‰) internal reversals (Fig. 17.5b), the large and abrupt positive excursion $\delta^{13}C_{org}$ (~5 ‰) confined to the Whitehill Formation (Fig. 17.5 a–c) makes this a distinct chemo-stratigraphic marker that can be traced as far as the Irati Formation in Brazil, with similar bio-, litho- and chemo-stratigraphy (du Toit 1926; Faure et al. 1995; Linol et al. 2016; Chap. 18 of this book). The $\delta^{13}C_{carbonate}$ values in the Whitehill Formation (Fig. 17.5d) are really low and are thus unlikely to be related to marine deposits. Assuming a freshwater origin, therefore, the $\delta^{13}C_{water}$ of the Karoo must have been extremely variable. Variability in $\delta^{13}C_{water}$ can probably explain the $\delta^{13}C_{org}$ variability without invoking a switch between different plant types or algal blooms

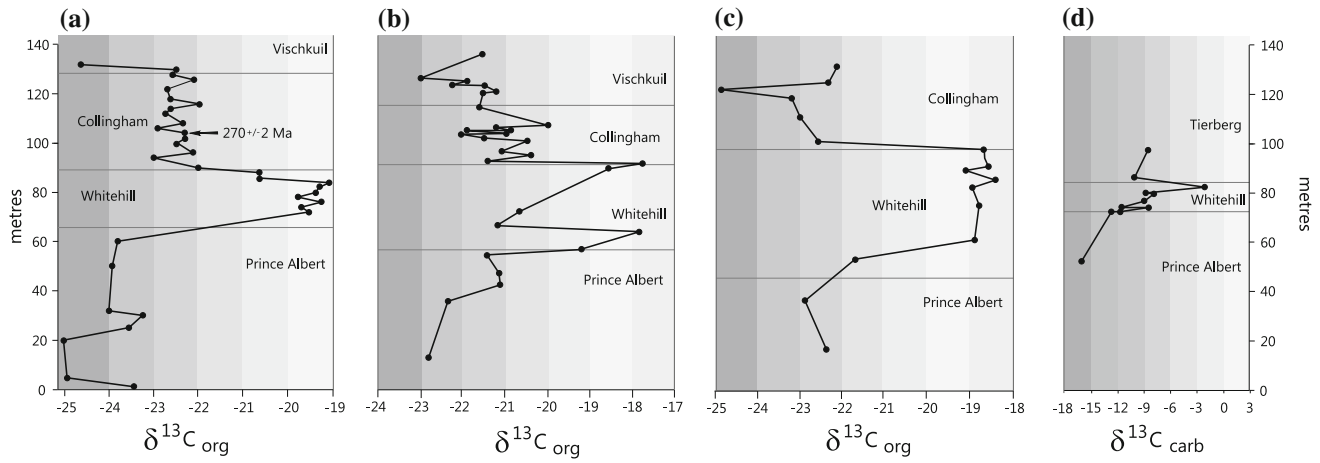

Fig. 17.5 Carbon isotope 'fingerprints' across the *black* gas-shales of the Whitehill Formation. $\delta^{13}C_{org}$ sections **a**–**c** are from sample areas 1, 4 and 5 shown on Fig. 17.2. The $\delta^{13}C_{carbonate}$ section **d** is from Faure et al. (1995). The origin for the distinct C-isotope perturbations across the Whitehill Formation remains to be resolved (see also Chap. 11 in this book)

(e.g., Faure et al. 1995). However, large $\delta^{13}C_{water}$ variations would also imply an isolated environment, closed from the atmosphere in, for example, a subglacial lake environment such as those found beneath present-day Antarctic ice sheets, such as Lake Vostok. This lake, which has been stable for 20 myrs, has a depth of up to 670 m beneath the ~4 km ice sheet of Antarctica and has accumulated up to several hundred metres of glacial sediments (Bell and Karl 1999; Siegert et al. 2001). Because the East Antarctic ice sheet flows across Lake Vostok (and at least 70 other large lakes that have now been identified beneath the ice; Jamieson et al. 2016), it acts as a conveyer belt delivering sediments to the lake bottom, as the base of the ice sheet melts during pressure release. This partial melting of the ice sheet is believed to supply sediments, new water, microbes and possibly gas hydrates to the lake (Bell and Karl 1999). Such an environment could explain the low spore/pollen counts in the lower Dwyka sequences of the southern Karoo.

17.8.2 Significant Shifts Across the P-T Boundary

The $\delta^{13}C_{org}$ shows significant fluctuations in the Upper Permian between −27 and −29 ‰, and a small negative spike (–30 ‰) is discernible (Fig. 17.3) around the P-T boundary. Lack of nodules throughout the section prevented identification of more pronounced spikes. However, there is a significant negative trend in the $\delta^{13}C_{org}$ from a mean around −23 ‰ between ~260 and 270 Ma. The general decline in $\delta^{13}C$ towards the P-T boundary and the general rapid fluctuation across the boundary have been linked to increasing exposure and oxidation of coals across the heartland of Gondwana, and release of methane gas from its continental margins (de Wit et al. 2002), as well as extensive gas emissions during the formation of the Siberian LIP (Svenson et al. 2009; Saunders 2016). But there is no overall agreement about cause and effects of the general decline and subsequent fluctuations across the Karoo P-T boundary (Faure et al. 1995; MacLeod et al. 2000; de Wit et al. 2002; Ward et al. 2005; Day et al. 2015; Gastaldo et al. 2015; Chap. 15 in this book).

17.8.3 Significant Shifts in the Upper Karoo

$\delta^{13}C_{org}$ values for all Molteno Formation samples typically range between −26 and −21 ‰ (Regime VIII; de Wit et al. in prep). Due to the wide range of values at well-sampled locations, no clear stratigraphic trend is observed. The greatest degree of variation occurs at the best-sampled location with well-preserved fossils representing riparian forest habitats. The spectrum of $\delta^{13}C_{org}$ values (for 13 samples) has a range of 4.3 ‰ (Fig. 17.2). Such a range of variation in $\delta^{13}C_{org}$ is greater than the 3.5 ‰ excursion in the $\delta^{3}C_{org}$ of wood observed across the Triassic-Jurassic (T-J) boundary elsewhere (Hesselbo et al. 2002).

Bulk rock (shale) and coal samples generally display isotopic ratios of a similar range, and within error of plant fossils. Isotopic variations do not follow taxonomic trends, supporting that bulk rock analysis is a reasonable alternative to fossil plant analysis when conducting $\delta^{13}C_{org}$ stratigraphy in the Upper Karoo Supergroup. All Molteno samples analysed show $\delta^{13}C_{org}$ values typical of modern C3 plants (Fig. 17.3), although all values lie within the higher end of the range of modern C3 plants, with a value of −24 ‰ (modern C3 plant average −27 ‰). The possible reasons for this are discussed elsewhere (Decker and de Wit 2005), but suffice it to state that the concentration of atmospheric CO_2 at this time was higher than it is today (Berner 1990), and the $\delta^{13}C$ value of atmospheric CO_2 in the Carnian (Molteno times) may have been higher than modern pre-industrial values. Alternatively, the data indicate high water use efficiency in Molteno plants, due to a saline or arid environment, and seasonal aridity may well have been a determining factor.

Details of the chemostratigraphy of the Elliot and Clarens Formations are discussed elsewhere (Decker 2004; Decker and de Wit 2005). $\delta^{13}C_{org}$ values oscillate relatively rapidly between −27 and −15 ‰, with at least seven episodic reversals (Fig. 17.3). The Elliot Formation is distinguished from the Molteno Formation chemostratigraphically by the existence of $\delta^{13}C_{org}$ values higher than −20 ‰. 30 % of the Elliot Formation samples have $\delta^{13}C_{org}$ values above −20 ‰ (Fig. 17.3). These values range as high as −16 ‰ (Decker and de Wit 2005) that occur as distinct, sharp, positive excursions. Most importantly, these positive excursions lie beyond the $\delta^{13}C$ range of modern C3 plants (Fig. 17.3), and have been interpreted as evidence of the episodic dominance of CAM plants (Crassulacean Acid Metabolism, also known as CAM photosynthesis) in response to severe episodes of drought during aridification towards a Jurrasic-Cretacous greenhouse world (Decker and de Wit 2005).

17.9 Discussion and Conclusions

Most, if not all of the Karoo sequences have terrestrial organic materials preserved suitable for Carbon isotope analysis. Organic Carbon isotope signatures ($\delta^{13}C_{org}$) across the Karoo sequences reveal distinct climate and ecosystem changes that can be tested against other stratigraphic observations especially fossils, to help reconstruct robust evolving paleoenvironments. But the work is in early stages and requires, and deserves, more detailed analyses to trace the terrestrial trends across Gondwana as has also been

attempted for India and Madagascar (e.g., Ghosh 1999; Rakatosolofo 1999; de Wit et al. 2002).

Following the formation of lacustrine conditions at the early Visean, Dwyka deposition may have occurred in a large subglacial lake similar to those reported beneath the modern Antarctic ice cap. There is only one recorded layer in the lowermost Prince Albert Formation that may represent a marine incursion, but even in this case, there is significant doubt about the environmental interpretation from this scanty fossil evidence (Ian McLachlan, pers comm 2001); and the stable isotope (carbon and sulphur) evidence to-date on this formation, favours a terrestrial saline lake environment during the immediate post-Dwyka period (Faure et al. 1995; Faure and Cole 1999; see also Chap. 11 in this book). Antarctic-like conditions clearly existed in source areas during deposition of the Dwyka sedimentation, as the South Pole traversed the Karoo (Opdyke et al. 2001; Preface this book). The Dwyka tillites and varves may therefore have formed in a lake, possibly episodically connected to marine waters, and perhaps similar to the present Antarctic subglacial Lake Vostok (Bell and Karl 1999; Siegert et al. 2001; Jamieson et al. 2016). Our field and stable-isotope data also confirm that there were significant interglacial episodes within the last 10 myrs of Dwyka deposition, as was postulated by Visser and Young (1990).

Wopfner (1999) has argued that deglaciation was extremely abrupt (<5 myrs) in the Late Asselian to Early Sakmarian, relatively consistent with the recent dating of the top of the Dwyka at about 290 Ma (Sakmarian-Artinskian transition; Bangert et al. 1999). The partial or total collapse of the ice sheet would in turn have contributed to global sea level rise during general global warming. The short marine incursion along the western part of the basin may represent a related sea level high-stand, but isostatic rebound after deglaciation may have kept the Karoo lake from becoming a large marine basin.

Deposition occurred predominantly in lacustrine environments; the size of the Karoo lake became gigantic following deglaciation, perhaps similar to the moraine blocked lake of the Baltic Sea following the last deglaciation and isostatic equilibration (Chap. 11 this book), which in turn re-established terrestrial conditions for the remained of the history of the interior of southern Africa.

The upper parts of the Karoo sequences contain two of the major extinction events (P-T and T-J) that now require further high resolution carbon isotope testing to reveal their global terrestrial connectivity to rapid, pulsating CO_2 (and related CH_4) emissions from large igneous provinces that are now precisely dated at around 252 Ma and 201 Ma, respectively (e.g., Hesselbo et al. 2002; Svensen et al. 2009; Schoene et al. 2010) as has been done successfully at resolutions well below 100,000 years elsewhere in marine systems (e.g., Ruhl et al. 2011; Burgess et al. 2014; Clarkson et al. 2015). Resolving the causes of the great decline of $\delta^{13}C_{org}$, some 3–4 million years ahead of the P-T boundary (Regime IV); and the large fluctuations well before the T-J boundary (Regime VIII) remain major challenges.

The transition into the Jurassic and Cretaceous hothouse environments is also well archived in the Karoo. Large fluctuations in the isotope ratios document the onset of severe droughts ahead of the onset of regional desertification that continued for at least 50 million years, as witnessed in Namibia, where dune fields, similar to those found intercalated with the lowermost lavas of the Drakensberg basalts in South Africa, are interbedded with the Lower Cretaceous Etendeka flood basalts (~132 Ma; Marsh et al. 2001). In addition, $\delta^{13}C_{org}$ of plant fossils across the T-J boundary have revealed nature's first engineering of CA photosynthesis. Thus, carbon isotope stratigraphy across the Karoo has shown the importance of chemical stratigraphy in unravelling its paleo-history. Combining this tool with other stable isotopes is now needed for a higher resolution.

Acknowledgments Funding for the studies was by NRF to MdW (Open Program). This chapter is a summary of a much more detailed manuscript that has been 'in progress' since 2004, and will be completed in due course. Thanks to B Linol for thorough reviews. This is AEON contribution number 161.

References

Ager DV (1973) The Nature of the Stratigraphic Record. Halsted (Wiley), New York, 114p. (3rd edition 1992, 151p).

Alexander J (1999) Carbon Isotope stratigraphy of Permo-Carboniferous sediments in the Karoo Basin, SE of Laingsburg, South Africa. Unpublished Hons. Thesis, University of Cape Town, 37p.

Anderson JM and Anderson HM (2003). The Heyday of the Gymnosperms: systematics and biodiversity of the Late Triassic Molteno fructifications. Strelitzia, 15, National Botanical Institute, Pretoria, 398p.

Anderson JM, Anderson HM, Archangelsky S, Bamford S, Chandra S, Dettman M, Hill R, Mcloughlin S and Rösler O (1999) Patterns of Gondwana plant colonisation and diversification. J Afr Earth Sci 28:145–168.

Bachtadse V, Van der Voo R and Halbich IW (1987) Paleomagnetism of the western Cape Fold Belt, South Africa, and its bearing on the Paleozoic apparent polar wander path for Gondwana. Earth Planet Sci Lett 84:487–499.

Bangert B, Stollhofen H, Lorenz V and Armstrong R (1999) The geochronology and significance of ashfall tuffs in the glaciogenic Carboniferous-Permian Dwyka Group of Namibia and South Africa. J Afr Earth Sci 29:33–50.

Bell RE and Karl DM (1999) Evolutionary processes a focus of Decade-long ecosysytem study of Antarctic's Lake Vostok. EOS, Trans Am Geophy Union 80:573–579.

Berner RA (1990) Atmospheric carbon dioxide levels over Phanerozoic time. Science 249:1382–1386.

Bordy EM, Hancox PJ, Rubidge BS (2004) Fluvial style variations in the Late Triassic–Early Jurassic Elliot Formation, main Karoo Basin, South Africa. J Afr Earth Sci 38:383–400.

Burgess, S.D., Bowring, S., and Shen, S.Z., 2014, High-precision timeline for Earth's most severe extinction. National Academy of Sciences Proceedings 111:3316–3321.

Clarkson et al. (2015) Ocean acidification and the Permo-Triassic mass extinction. Science 348:229–232.

Day MO, Ramezani J, Bowring SA, Sadler PM, Erwin DH, Abdala F and Rubidge BS (2015) When and how did the terrestrial mid-Permian mass extinction occur? Evidence from the tetrapod record of the Karoo Basin, South Africa. Proc R Soc B 20150834.

Decker JE (2004) Organic Carbon Isotope Stratigraphy of the Mesozoic Upper Karoo Supergroup, Main Karoo Basin, South Africa, in a Seismic Stratigraphic Framework. Unpublished M.Sc. thesis, University of Cape Town, 144p.

Decker JE and de Wit MJ (2005) Carbon isotope evidence for CAM photosynthesis in the Mesozoic. Terra Nova 18:9–17.

De Wit MJ, Ghosh JG, de Villiers S, Rakotosolofo N, Aexander J, Tripathi A and Looy C (2002) Multiple organic carbon isotope reversals across the Permo-Triassic boundary of terrestrial Gondwana sequences: Clues to extinction patterns and delayed ecosystem. J Geol 110:227–24.

Duncan RA, Hooper PR, Rehacek J, Marsh JS, Duncan AR (1997) The timing and duration of the Karoo igneous event, southern Gondwana. J Geophys Res 102:18127–18138.

Du Toit AL (1926) The Geology of South Africa (*3rd edition, 1954*). Oliver and Boyd, Edinburgh.

Faure K, de Wit MJ and Willis JP (1995) Late Permian global coal hiatus linked to ^{13}C depleted CO_2 flux into the atmosphere during the final consolidation of Pangea. Geology 23:507–510.

Faure K and Cole D (1999) Geochemical evidence for lacustrine microbial blooms in the vast Permian Main Karoo, Paraná, Falkland Islands and Haub basins of southwestern Gondwana. Palaeogeogr Palaeoclimatol Palaeoecol 152:189–213.

Fildani A, Drinkwater NJ, Weislogel A, McHargue T, Hodgson DM and Flint SS (2007) Age controls on the Tanqua and Laingsburg deep-water systems: new insights on the evolution and sedimentary fi ll of the Karoo basin, South Africa. J Sediment Res 77:901–908.

Gastaldo RA, Kamo SL, Neveling J, Geissman JW, Bamford M and Looy CV (2015) Is the vertebrate-defined Permian-Triassic boundary in the Karoo Basin, South Africa, the terrestrial expression of the end-Permian marine event? Geology 43:939–942.

Geel C, de Wit M, Booth P, Schulz H-M and Horsfield B (2015) Palaeo-environment, diagenesis and characteristics of Permian black shales in the Lower Karoo Supergroup flanking the Cape Fold Belt near Jansenville, eastern Cape, South Africa: Implications for the shale gas potential of the Karoo Basin. S Afr J Geol 118:249–274.

Ghosh JG (1999) U/Pb geochronology and structural geology across major shear zones of the southern granulite terrain of India and the $\delta^{13}C_{org}$ stratigraphy of the Gondwana coal basins of India: their implication for Gondwana studies. Unpublished PhD thesis, University of Cape Town.

Grossman, E.L. 1994. The carbon and oxygen isotope record during the evolution of Pangea: Carboniferous to Triassic. Geol Soc Am Spec Pap 288:207–228.

Hessselbo SP, Robinson SA, Surlyk F and Piasecki S (2002) Terrestrial and marine extinction at the Triassic-Jurassic boundary synchronized with major carbon-cycle perturbation: A link to initiation of massive volcanism? *Geology* **30**: 251–254.

Higgs R (2010) Comments on 'Sequence stratigraphy of an argillaceous, deepwater basin plain succession: Vischkuil Formation (Permian), Karoo Basin, South Africa' from van der Merwe, Flint and Hodgson (Mar Pet Geol 27: 321–333). Mar Pet Geol 27:2073-2075.

Jamieson SSR, Ross N, Greenbaum JS, Young DA, Aitken ARA, Roberts JL, Blankenship DD, Bo S and Siegert MJ (2016) An extensive subglacial lake and canyon system in Princess Elizabeth Land, East Antarctica. Geology 44:87–90.

Jenkyns HC, Jones CE, Gröke DR, Hesselbo SP and Parkinson DN (2002) Chemostratigraphy of the Jurassic System: applications, limitations and implications for palaeoceanography. J Geol Soc London 159:351–378.

Johnson MR et al. (1997) The Foreland Karoo Basin, South Africa. In: Selley RC (ed) African basins. Sedimentary basins of the World. Elsevier, Amsterdam, pp. 269–317.

Knütter RKC, Fiedler K, Adelman D, Albes D, Zechner J (1995) Geological map of Laingsburg area, 1:25000, Bonn University Unpublished.

Linol B, de Wit MJ, Barton E, de Wit MCJ and Guillocheau F (2016) U–Pb detrital zircon dates and source provenance analysis of Phanerozoic sequences of the Congo Basin, central Gondwana. Gondwana Res 29:208–219.

Marsh JS, Ewart A, Milner SC, Duncan AR and Miller RMcG (2001) The Etendeka Igneous Province: magma types and their stratigraphic distribution with implications for the evolution of the Parana- Etendeka flood basalt province. Bull Volcanol 62:464–486.

McCabe C and Elmore RD (1989) The occurrence and origin of Late Paleozoic remagnitisation in the sedimentary rocks of North America. Rev Geophys 27:471–494.

MacLeod KG, Smith RMH, Koch PL and Ward PD (2000) Timing of mammal-like reptile extinctions across the Permian-Triassic boundary in South Africa. Geology 28:227–230.

McLachlan IR and Anderson AM (1973) A review of the evidence for marine conditions in southern Africa during Dwyka times. Palaeontologica Africana 15:37–64.

McKay MP, Weislogel AL, Fildani A, Brunt RL, Hodgson DM and Flint SS (2015) U-PB zircon tuff geochronology from the Karoo Basin, South Africa: implications of zircon recycling on stratigraphic age controls. Int Geol Rev 57:393–410.

Mii H-S, Grossman EL, Yancey TE, Chuvashow B and Egorov A (2001) Isotopic records of brachiopod shells from the Russian Platform – evidence for the onset of mid-Carboniferous glaciation. Chem Geol 175:133–147.

Opdyke ND, Mushayandebun M and de Wit MJ (2001) A new palaeomagnetic pole for the Dwyka System and correlative sediments in sub-Saharan Africa. J Afr Earth Sci 33:143–154.

Plumstead EP (1964) Gondwana floras, geochronology and glaciation in South Africa. International Geological Congress, 22nd Session, India, pp. 303–319.

Rakotosolofo NA (1999) Geology, Carbon isotope stratigraphy, and palaeomagnetism of the Karoo sequences of the southern Morondava basin, SW Madagascar. Unpublished MSc. thesis, University of Johannesburg (formerly Rand Afrikaans University).

Raymo ME (1994) The initiation of northern hemisphere glaciation. Ann Rev Earth Planet Sci 22:353–383.

Ruddiman WF (2000) Earth's Climate. W H Freeman & Co. NY, 465p.

Rubidge BS, Erwin DH, Ramezani J, Bowring SA and de Klerk WJ (2013) High-precision temporal calibration of Late Permian vertebrate biostratigraphy: U-Pb zircon constraints from the Karoo Supergroup, South Africa. Geology 41:363–366.

Ruhl M, Bonis NR, Reichart G-J, Damsté JSS, Kürschner WM (2011) Atmospheric Carbon Injection Linked to End-Triassic Mass Extinction. Science 333:430–434.

Saltzman MR, González LA and Lohmann KC (2000) Earliest carboniferous cooling step triggered by the Antler orogeny? Geology 28:347–350.

Saunders AD 2016. Two LIPs and two Earth-system crises: the impact of the North Atlantic Igneous Province and the Siberian Traps on the Earth-surface carbon cycle. Geol Mag 153.

Schoene B, Guex J, Bartolini A, Schaltegger U and Blackburn TJ (2010) Correlating the end-Triassic mass extinction and flood basalt volcanism at the 100 ka level. Geology 38:387–390.

Scott AC, Anderson JM and Anderson HM (2004) Evidence of plant–insect interactions in the Upper Triassic Molteno Formation of South Africa. J Geol Soc London 161:401–410.

Siegert MJ, Ellis-Evans JC, Tranter M, Mayer C, Petit J-R, Salamatin A and Priscu JC (2001) Physical, chemical and biological process in Lake Vostok and other subglacial lakes. Nature 414:603–609.

Smith AG (1999) Gondwana: its shape, size and position from Cambrian to Triassic times. J Afr Earth Sci 28:71–97.

Smith RMH, Erickson PA and Botha WJ (1993) A review of the stratigraphy and sedimentary environments of the Karoo-aged basins of southern Africa. J Afr Earth Sci 16:143–169.

Streel M and Theron JN (1999) The Devonian-Carboniferous boundary in South Africa and the age of the earliest episode of the Dwyka glaciation: New palynological result. Episodes, 22:41–44.

Svensen SH, et al. (2009) Siberian gas venting and the end-Permian environmental crisis. Earth Planet Sci Lett 277:490–500.

Thackeray J F, van der Merwe NJ, Lee-Thorpe JA, Sillen A, Lanham J L, Smith R, Keyser A and Monteiro PMF (1990). Carbon isotope evidence for Late Permian therapsids teeth, for a progressive change in atmospheric CO2 composition. Nature 347:751–753.

Turner BR (1983) Braidplain deposition of the Upper Triassic Molteno Formation in the main Karoo (Gondwana) Basin, South Africa. Sedimentology 30:77–89.

Turner BR (1999) Tectonostratigraphical development of the upper Karoo foreland basin: orogenic unloading versus thermally-induced Gondwana rifting. J Afr Earth Sci 28:215–238.

Veevers JJ, Cole DI, Cowan EJ (1994) Southern Africa: Karoo Basin and Cape Fold Belt. In: Veevers, J.J., Powell, McA. (Eds) Permian-Triassic Pangean Basins and foldbelts along the Panthalassan margin of Gondwanaland. Geol Soc Am Mem 184:223–280.

Veizer J *et al*. (1999) $^{87}Sr/^{86}Sr$, $\delta^{13}C$ and $\delta^{18}O$ evolution of Phanerozoic sea water. Chem Geol 161:59–88.

Visser JNJ (1987) The Palaeogeography of part of southwestern Gondwana during the Perm-Carboniferous glaciation. Paleogeogr Palaeoclimat Palaeoecol 61:205–219.

Visser JNJ and Young GM (1990) Major element geochemistry and paleoclimatology of the Permo-Carboniferous glacigene Dwyka Formation and post-glacial mudrocks in southern Africa. Palaeogeogr Palaeoclimat Palaeoecol 81:49–57.

Ward PD, Botha J, Buick R, DeKock MO, Erwin DH, Garrison GH, Kirschvink JL and Smith R (2005) Abrupt and Gradual extinction among Late Permian land vertebrates in the Karoo Basin, South Africa. Science 307:709–714.

Wopfner H (1999) The Early Permian deglaciation event between East Africa and northwestern Australia. J Afr Earth Sci 29:77–90.

Zawada PK (1988) Trace elements as possible paleosalinity indicators for the Ecca and Beaufort Group mudrocks in the southwestern Orange Free State. S Afr J Geol 91:18–26.